Magnetization of uniform Josephson junctions

D.-X. Chen and A. Hernando
Instituto de Magnetismo Aplicado, Red Nacional de Ferrocarriles Españoles-Universidad Complutense de Madrid (RENFE-UCM), P.O. Box 155, 28230 Las Rozas, Madrid, Spain
(Received 29 July 1993)

The magnetization curves and phase, field, and current-density profiles for uniform Josephson junctions (JJs) with length $2L$ are calculated from the sine-Gordon equation. It is found that M starts to be a multivalued function of H at $l \equiv L/\lambda_J = l_c = 1.995$, λ_J being the Josephson penetration depth; when $l > l_c$, increasing and decreasing H will cause M to jump so that hysteresis loops are formed; the hysteresis loops of very long JJs with $l \gg l_c$ have a shape similar to that of type-II superconductors (SC2s) with a surface barrier but both have quantitative differences; being cooled in a constant field, JJs show a Meissner effect distinct from that of SC2s. These results are explained in terms of Josephson vortices. One of the most fundamental differences between JJs and SC2s is that there is a surface current separated from the vortices for the latter but not for the former.

I. INTRODUCTION

Josephson[1] derived his dc and ac equations to describe the electromagnetic properties of a system consisting of two superconductors weakly linked across a thin insulating layer. The linked part is now called a Josephson junction (JJ), and the phenomena directly connected to these equations are referred to as the dc and ac Josephson effects. Such junctions are usually classified into two types, short (narrow) and long (wide), discriminated by the ratio $l \equiv L/\lambda_J$, where $2L$ and λ_J are the length and penetration depth of the junction, to be less or greater than 0.5. For short JJs the field produced by the currents flowing through them has a negligible influence on their properties; on the contrary, the self-field effect has to be considered for long JJs.

Considering a gauge-invariant phase difference, the dc Josephson equation for JJs in a uniform applied field parallel to the junction plane and perpendicular to the junction length results in a sine-Gordon equation which contains λ_J.[1-7] Analytic solutions of this latter equation have been given by a number of authors.[1-6] It is reduced to a first-order linear differential equation for short JJs because their λ_J can be regarded as infinite. Its solution for the transport critical current as a function of the applied field has the form of the Fraunhofer diffraction pattern[6] in physical optics. For long JJs, however, the solutions are in general multivalued, consisting of elliptic integrals. Concerning their magnetic properties, Kulik[3] has made systematic derivations for the case of $l \to \infty$, giving the equilibrium magnetization curve. For the case of finite l, transport properties have been computed by Owen and Scalapino,[5] and some magnetization curves, $M(H)$, were obtained by Yamashita and Rinderer[7] experimentally based on a mechanical analog model. Knowledge of the magnetization of uniform JJs has up to now been gained from these theoretical or semitheoretical works.

In this paper, we will extend this knowledge by systematic and accurate computations directly from the sine-Gordon equation. The l range is chosen to be as wide as necessary and possible (from 0.25 to 20). No external current is applied to the JJ so that the subject can be referred to as the magnetization of JJs. Since it is difficult to envisage precisely the magnetic properties of JJs without detailed computations, some important features of JJs were ignored up to now. They are studied in this work.

The model and mathematics are introduced in Sec. II. Some computed results are given in Sec. III with preliminary phenomenological analyses. The magnetization is further described in Sec. IV. Following tradition, our presentation will be parallel to the magnetization of type-II superconductors (SC2s). Since the similarities between long JJs and SC2s have been universally emphasized in the literature, we are mainly concerned with the unique properties of JJs and the essential differences between both. The conclusions are given in Sec. V.

II. MODEL AND MATHEMATICS

Let us consider a uniform junction J between two bulk superconductors S_1 and S_2, as shown in Fig. 1. The length of the junction, along the y axis, is $2L$; its thickness, along the x axis, is $2d = 2\lambda_L + t$, where λ_L is the London penetration depth of the superconductors and t is the thickness of the insulating layer. A uniform magnetic field H is applied along the z dimension of the assembly, which is infinite so that there is no demagnetizing field.

Upon applying H below the lower critical field H_{c1} of the superconductors, two kinds of currents, circulating in S_1 and S_2 and in J, appear. The magnetization M of the junction is provided by the latter. Owing to the infinite z dimension, currents are uniform along the z axis and the field produced by the currents has a z component only, which is also uniform along the same axis. Moreover, taking the original point of the coordinates as the center of the junction, the currents flowing along the y axis can be equated with those flowing in two infinitely thin sheets on the planes of $x = \pm d$, so that the internal field H_i between these sheets becomes independent of the x coordinate. Thus, the problem turns out to be one dimensional.

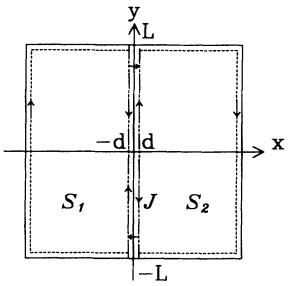

FIG. 1. Schematic of a Josephson junction assembly. The junction J is bordered by two long-dashed lines. The circulating currents in S_1 and S_2 are shown by short-dashed lines, on each of which there are two arrows pointing in the clockwise direction of current. The other four arrows within J and its border represent the junction currents. Applied field is along the z axis.

For the sake of simplicity, dimensionless quantities are defined for L, y, H, H_i, and M as

$$l\equiv\frac{L}{\lambda_J},\quad \eta\equiv\frac{y}{\lambda_J},\quad h\equiv\frac{H}{H^*},\quad h_i\equiv\frac{H_i}{H^*},\quad m\equiv\frac{M}{H^*}\ , \tag{1}$$

with

$$\lambda_J\equiv\sqrt{\Phi_0/4\pi\mu_0 J_0 d}\ , \tag{2a}$$

$$H^*\equiv\Phi_0/4\pi\mu_0\lambda_J d\ , \tag{2b}$$

where Φ_0 is the flux quantum and J_0 is the maximum tunneling current density at zero field. Thus, the sine-Gordon equation for the gauge-invariant phase difference θ can be written as[3]

$$d^2\theta/d\eta^2=\sin\theta\ , \tag{3a}$$

with

$$d\theta/d\eta=h_i\ . \tag{3b}$$

Owing to the symmetry, we only need to consider one-half of the junction, whose boundary conditions are

$$\theta=0 \text{ for } \eta=0\ , \tag{4a}$$

$$h_i=h \text{ for } \eta=l\ . \tag{4b}$$

The solution of Eq. (3a) with condition (4a) is[3]

$$\eta=\frac{1}{2}\int_0^\theta\frac{d\theta'}{\sqrt{\sin^2(\theta'/2)+a^2}}\ , \tag{5}$$

where a is a constant to be determined by condition (4b). For computation, Eq. (5) is further expressed in terms of elliptic integrals as

$$\eta=k\{n'K(k)+(-1)^nF[(-1)^n(\theta-n'\pi)/2,k]\}\ , \tag{6}$$

where K and F denote complete and incomplete elliptic integrals of the first kind. The argument

$$k=(1+a^2)^{-1/2}\ , \tag{7}$$

n is the maximum integer less than $\theta/\pi+1$, and $n'=n-[1+(-1)^n]/2$.

The computations are carried out with a MATHEMATICA program, aimed at obtaining an $a(\theta_l)$ function, where θ_l is the θ at $\eta=l$, that satisfies condition (4b) for a given l with an accuracy better than 0.01%. Having $a(\theta_l)$, $m(h)$ is computed using

$$h=2\sqrt{\sin^2(\theta_l/2)+a^2}\ , \tag{8a}$$

$$m=b/\mu_0-h=\theta_l/l-h\ . \tag{8b}$$

These two equations are derived from Eqs. (3b) and (4b), and b is the averaged flux density B of the junction normalized to H^*.

The profiles of phase, internal field, and current density can also be obtained after obtaining $a(\theta_l)$. Changing θ stepwise from zero to a given θ_l, $\theta(\eta)$ is computed from Eqs. (6) and (7). This function leads directly to $h_i(\eta)$ using Eq. (8a) whose h and θ_l are replaced by h_i and θ, respectively. The normalized current density $j\equiv J/J_0$, where J is the current density, is then calculated from the original dc equation

$$j=\sin\theta\ . \tag{9}$$

III. COMPUTATION RESULTS

A. Magnetization curves

The computed $m(h)$ curves for $l=0.5$, 1, 2, 4, 8, 12, 16, and 20 are plotted in Figs. 2(a)–2(h) successively. We see that m oscillates around the h axis for all the curves, which is a natural consequence of the sine function in Eq. (3a). By measuring the distance between the points where $m=0$ and defining the h period as $(\Delta h)_j=h_{j+2}-h_j$, where h_j is h at the jth zero-m point counted from 0 at $h=m=0$, we have

$$(\Delta h)_j=2\pi/l \text{ for } j\geq 1\ . \tag{10}$$

This equality is not exact but very accurate for large j. Examining carefully the values for small j, we find that if $l=2$, the error of Eq. (10) is within $\pm 0.4\%$. For $l<2$, the actual $(\Delta h)_j$ can be $\sim 1.5\%$ greater if $j=1$, but this error decreases quickly with increasing j. The situation for $l>2$ is different, where the error of calculated $(\Delta h)_j$ is negative at small j. The largest error is around -5% at $j=1$, and it changes slowly with increasing j if l is large.

Thus, $l=2$ serves as a critical case that separates the positive and negative errors of Eq. (10). It also divides the $m(h)$ curves into two types. m is a multivalued function of h if $l>2$ but it is single valued if $l<2$.

B. Phase, field, and current-density profiles

To show the phase, field, and current-density profiles we have to define some typical cases. We choose four values of l which in logarithmic scale are symmetrically located on either side of the critical case of $l=2$. Such an l range also covers the lengths of most practical short and long JJs, and its lower and upper limits can be well compared with the ideal cases of $l\to 0$ and ∞. Moreover, we choose θ_l to be $\pi/2$ multiplied by small integral numbers in order to simplify the plots. Thus, in Figs. 3, 4, 5,

and 6, we show (a) $\theta(\eta)$, (b) $h_i(\eta)$, and (c) $j(\eta)$ profiles for $l=0.25$, 1, 4, and 16, respectively, at $\theta_l=i\pi/2$, $i=1,2,3,\ldots,8$.

The profiles for $l=0.25$ given in Fig. 3 are practically the same as the ideal ones for $l\to 0$. The h_i is constant against η, which means that the field produced by currents is negligible. θ is a linear function of η, resulting from the integration of constant h_i. The profile of j is always a part of sinusoidal function of η, as easily visualized from Eq. (9) and a linear $\theta(\eta)$. In other words, a JJ of $l=0.25$ is a typical short one.

On the other hand, one can see the departure of the results for $l=1$ given in Fig. 4 from those for $l\to 0$ described above. This departure can be easily observed from the h_i profiles; they are no longer flat. According to the traditional classification, this JJ of $l=1$ is a long one.

The trend of change in the profiles continues for even greater l. We see wave-shaped $h_i(\eta)$ and severely nonlinear $\theta(\eta)$ for $l=4$ in Fig. 5. However, it is interesting that the wave forms of $j(\eta)$ are not sensitive to l even when it is increased to 4. For $\theta_l=4\pi$, $j(\eta)$ is still very close to sinusoidal. Only when θ_l is small, can one see it tilted towards the JJ edge ($\eta=l$).

Tremendous changes occur for all three profiles when $l=16$ as seen from Fig. 6. θ shows stages, h_i becomes peaks, and $j(\eta)$ has a unique shape close to $dh_i(\eta)/d\eta$. These should be characteristic features of very long JJs, which will be our main concern in this work.

In the cases of $\theta_l=4\pi$, two field and current periods are present as long as we are able to see the periodic feature. These two periods are exactly identical. For $2\pi<\theta_l<4\pi$, there is a fractional period besides the complete one; the former is exactly a part of the latter. Such accurate periodicity is also ascribed to the sine function in Eq. (3a).

We should emphasize that all these profiles are calculated for low fields (or small θ_l). Increasing θ_l for larger l will result in the profiles approaching those for smaller l, although the number of periods will be greater.

IV. JOSEPHSON JUNCTION MAGNETIZATION

A. Initial susceptibility

After describing in Sec. II some phenomena appearing in the $m(h)$ curves and the profiles, we now come to deeper and quantitative physics, i.e., the Josephson junction magnetization. We start with the simplest property,

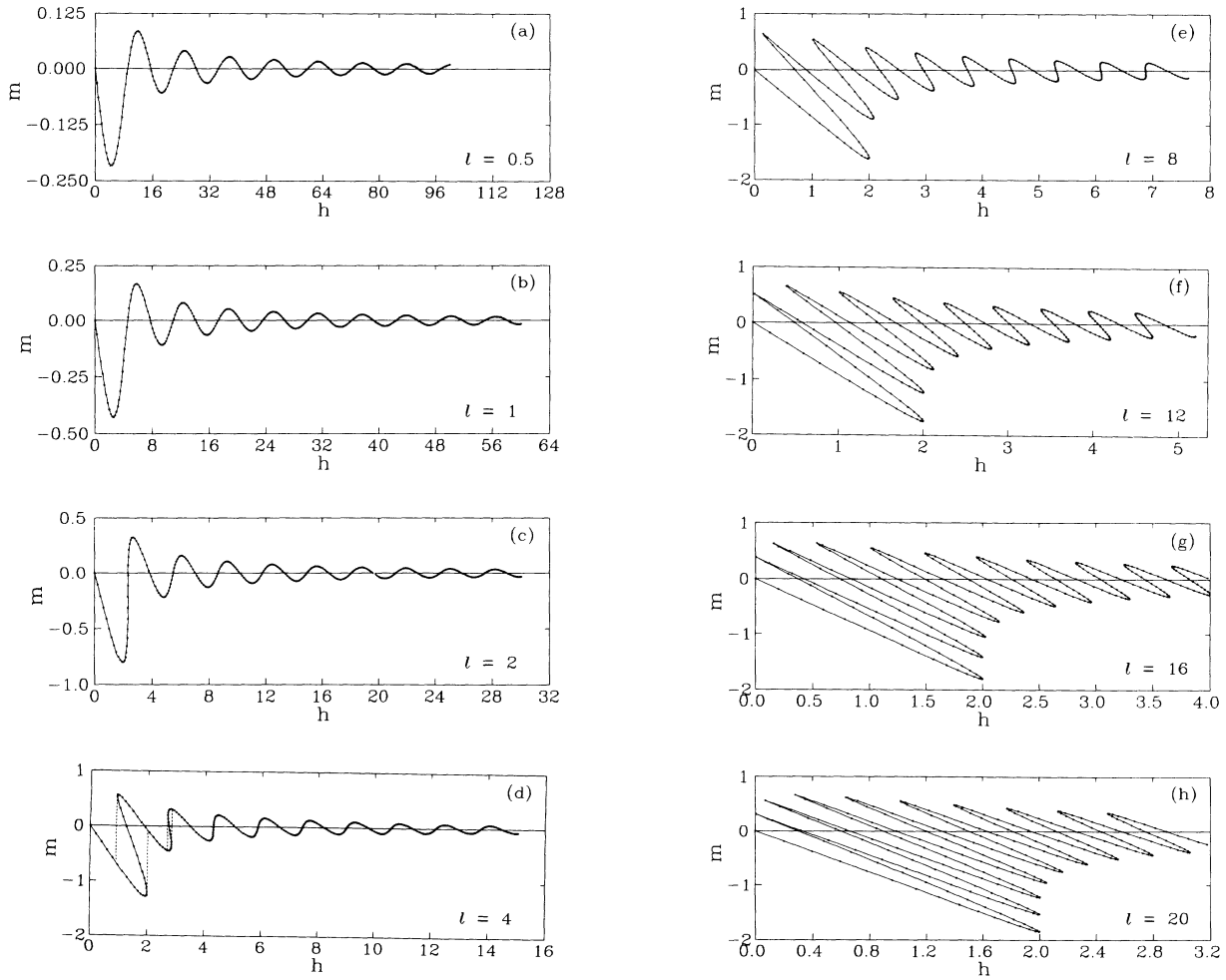

FIG. 2. Computed $m(h)$ curves for $l=0.5$ (a), 1 (b), 2 (c), 4 (d), 8 (e), 12 (f), 16 (g), and 20 (h).

namely, the initial susceptibility, $\chi_{\rm ini}$. It can be observed from Fig. 2 that the initial slope of the $m(h)$ curve decreases with increasing l. It follows, with an accuracy better than 0.1% in computations with finer θ_l steps, that

$$\chi_{\rm ini} \equiv (dm/dh)_{h=0} = l^{-1}\tanh l - 1 \ . \tag{11}$$

This equation can be obtained by solving Eq. (3a) with $\sin\theta$ replaced by θ under the boundary conditions $h_i(l)=h_i(-l)=h$ and using Eq. (8b). Therefore, the 0.1% can be regarded as the maximum computation error for the field.

Actually, this $\chi_{\rm ini}$ is the same as that for an infinite slab of SC2 in the Meissner regime,[8] owing to the exponential decay of field from the surfaces. In Figs. 3–6, we did not show h_i profiles for very small h or θ_l. But the $h_i(\eta)$ curves for $\theta_l=\pi/2$ in Figs. 5(b) and 6(b) are rather close to exponential.

In our model, the three circulating currents at very small h in a very long JJ assembly can be equated with one closed current sheet, as shown in Fig. 7(a). In S_1 and S_2 it is distant from the surfaces by λ_L, whereas in J, by λ_J.

B. Josephson vortices

The second property of JJs concerns the periodic nature of the field and current profiles, namely the presence of Josephson vortices (JVs). Because of the importance of this feature it has been emphasized in most of the existing works on long JJs, and so we give it priority over the rest.

As for the Abrikosov vortex (AV) in SC2s, the concept

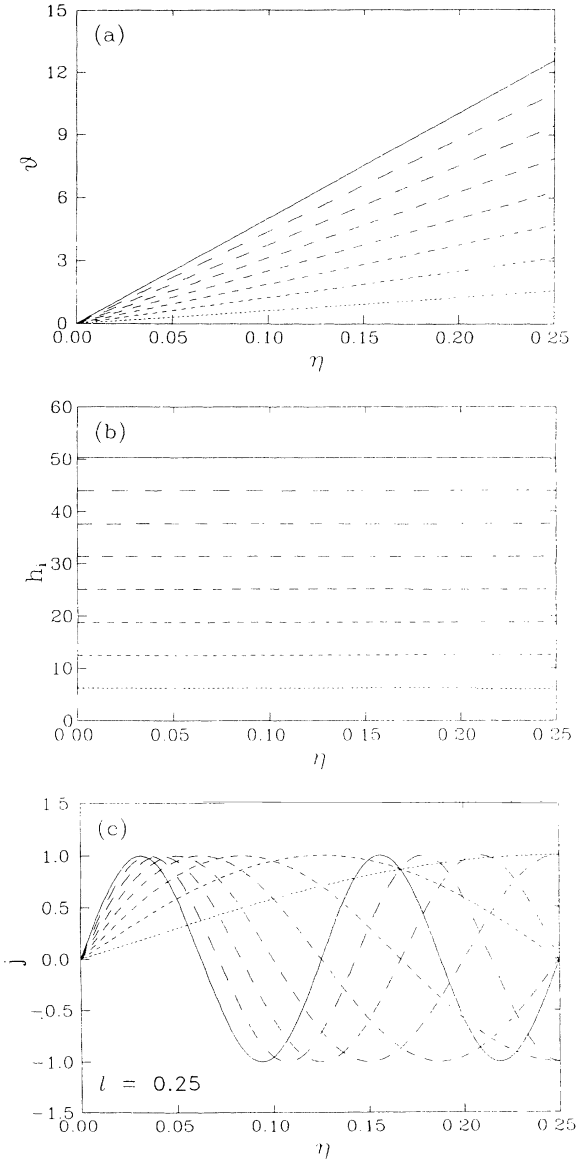

FIG. 3. The $\theta(\eta)$ (a), $h_i(\eta)$ (b), and $j(\eta)$ (c) profiles for $l=0.25$. In each case, eight curves from the very-short-dashed line to the solid line are for $\theta_l/\pi=0.5$, 1, 1.5, 2, 2.5, 3, 3.5, and 4, respectively.

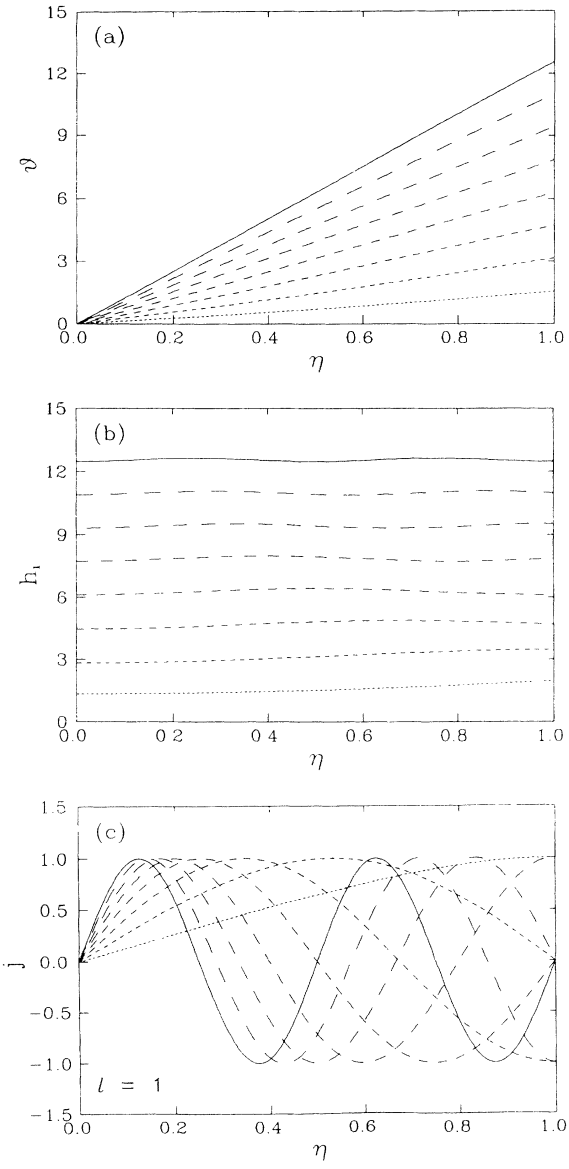

FIG. 4. Same as Fig. 3, but $l=1$.

of the JV was introduced by solving Eq. (3a) for $l \to \infty$. The solution has a soliton type, h_i taking a maximum at $\eta=0$ and being equal to zero when $\eta=l$:

$$\theta=4\arctan e^{\eta} . \tag{12}$$

It gives $\theta(-l)=0$, $\theta(l)=2\pi$, and $\theta(0)=\pi$. Obviously, this JV contains one Φ_0 of magnetic flux since the entire change in phase difference is 2π. Its field and current-density profiles are almost identical to those shown in Figs. 6(b) and 6(c) for $\theta_l=2\pi$ but with two differences as follows: (1) The latter are centered at $\eta=8$ but not 0 because in their calculation θ at the center has been chosen as 0 but not π. (2) There is an unobservable difference in the profile shapes since Eq. (12) implies that $a=0$ but in the other case $a=0.001\,32$.

Analogous to the single JV in an infinite JJ, the JV in a finite JJ should be defined as a current vortex associated with a field peak whose total flux equals Φ_0. From Figs. 5 and 6, we see that $\eta=0$ is always the border of a JV. The total number of JVs in the half of JJ is defined as

$$n_v=\theta_l/2\pi . \tag{13}$$

If n_v is an integer, there exist complete JVs only; otherwise, we have an incomplete JV cut by the JJ edge.

In Fig. 7(b), we draw a schematical JV structure for a JJ containing two JVs whose fields are along the applied field, as in the case of $l=16$ and $\theta_l=2\pi$ shown in Fig. 6. Two schematical figures of JV structure in long JJs are found in the literature, both having different features than shown in Fig. 7(b). Figure 19 of Ref. 4 shows a structure containing three JVs, one being at the junction center and the other two on each side. On the other

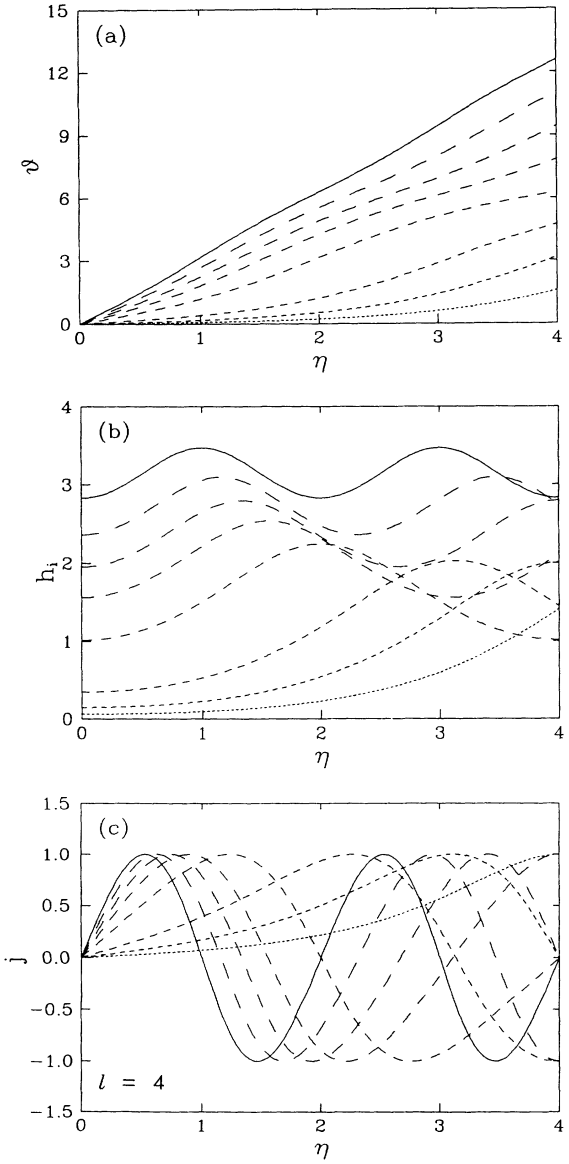

FIG. 5. Same as Fig. 3, but $l=4$.

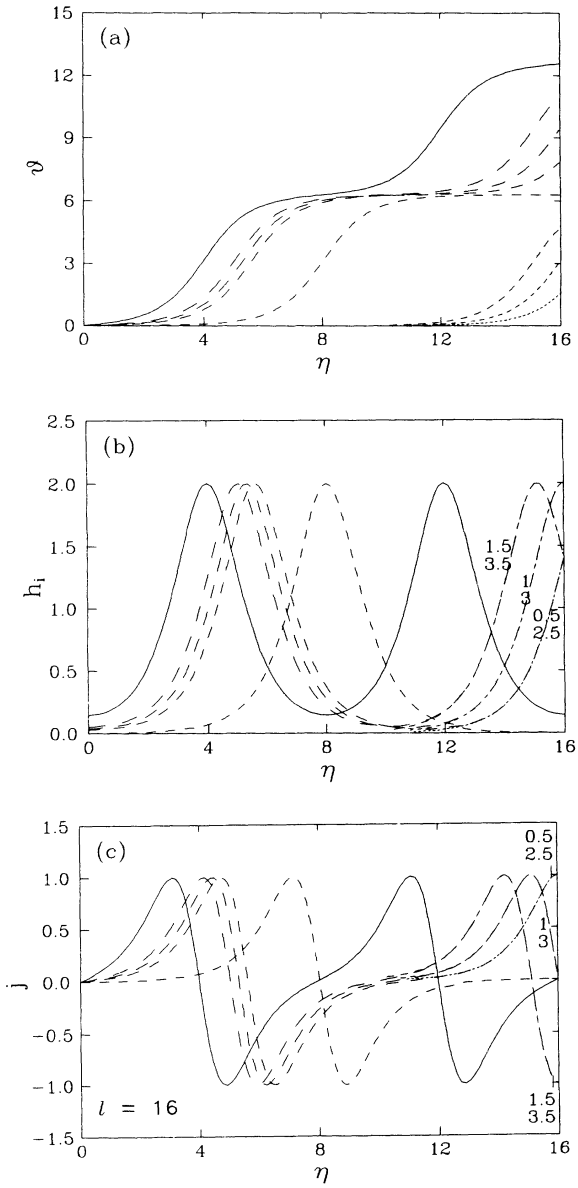

FIG. 6. Same as Fig. 3, but $l=16$. For overlapped curves, θ_l/π values are indicated. The data are not available for $\theta_l/\pi \leq 1.5$ and $\eta < 10$.

hand, Fig. 149 of Ref. 6 draws two JVs located at either half of the JJ, both giving fields opposite to the applied field. We note that all three cases concern static magnetic properties only, no transport current being applied. The above definition of a JV in finite JJs is valid for all the three configurations. However, careful analyses on the three will lead to a deeper insight into the nature of JVs, and thereby it turns out that some additional properties have to be attached to them.

The illustration in Ref. 4 is consistent with the soliton solution since in both cases a JV is centered at the JJ. To obtain such a solution one has to assume $\theta=\pi$ at the center instead of 0. This is also acceptable considering the symmetry, but it is not realistic since it will introduce an overly high energy to the JJ compared with the case of $\theta(0)=0$. Actually, the current induced by small fields always produces a field opposing the applied field, thus shielding the interior. Such a state has a lower energy than that with a centered JV since both the average field and current associated with two fractional edge JVs are smaller than those of an almost complete JV at the center. With increasing field, the two fractional JVs, which carry fields in the same direction as the applied field, become larger and form two complete ones. Therefore, the configuration in Ref. 6 is not realistic and the field carried by the JVs should have the same direction as the applied field.

Thus, we can add two properties to the JVs in uniform JJs that are not subjected to a transport current: (1) The field carried by JVs always points in the direction of the applied field, and (2) a JV can never form at the JJ center. We have argued these from the process of the first JV formation, but similar arguments can be made for any other cases. Therefore, these properties are in general valid.

JVs in a JJ have another important property: (3) There are no distance and overlap between two adjacent JVs even if one of them is fractional. This follows directly from the periodicity of the h_i and j profiles; the periods are continuous.

Adding these three properties, JVs defined in this way are still not the ones that are of common concern. The reason is that the above definition is valid for *all* uniform JJs regardless of whether they are short or long. Traditionally, the concept of JVs is used for long JJs only, when they are analogous to SC2s.[1-7] Universally defined JVs can be used for some particular cases only; this implies that some important characteristics of the JVs must have been overlooked, and without a further specification their applications would involve errors. At this point, we switch our topic to the properties of long JJs.

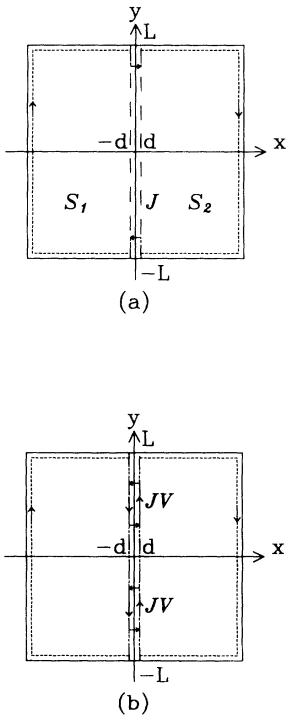

FIG. 7. (a) Low-field shielding state. (b) A state with two complete JVs. Applied field is along the z axis.

C. Magnetic irreversibility

As mentioned in Sec. III, when l is greater than 2, m becomes a multivalued function of h. This means that at a given value of h there can be several different states possible. The energies of these states are different since they contain different numbers of JVs. For example in Fig. 6 for the case of $l=16$, the states containing 0.25, 0.75, 1.25, and 1.75 JVs correspond to the values of h very close to 1.41. If fixing the h as 1.41, these n_v's should be almost unchanged. The lowest energy is for $n_v=0.25$. Since these states are not continuous, movement from one to another will undergo an m jump. During the jump, the JJ is not in equilibrium and its supercurrent-bearing ability is surpassed; i.e., the ac Josephson effect will play its part accompanied by high-frequency oscillations and energy losses. We will not consider the ac effect in more detail but simply use the m jumps to represent it. In reality, such jumps do not occur everywhere. When we sweep h up and down, the magnetic state (h,m) will always follow the continuous $m(h)$ curve unless h reaches its local maximum or minimum where (h,m) jumps to the nearest point on the same curve with the same h. The magnetization process is reversible when following the $m(h)$ curve but irreversible when undergoing an m jump.

We have used 2 as the critical l, below which there is no existing irreversibility in the magnetization. Writing this l as l_c, it can be determined with higher precision by detailed computations as

$$l_c=1.995\ , \tag{14}$$

which corresponds to a first jump occurring at $h=h_c=2.319$, where $m=-0.239$ and $\theta_l=4.15$. These not-simple numbers suggest that the value of l_c would be difficult to obtain analytically.

We now argue that when $l\approx l_c$ the influences from the self-field and the applied field can be regarded as being balanced. At very low h, the self-field opposes h and tends to decrease $\chi_{\rm ini}$ from 0 to -1. We can use this $\chi_{\rm ini}$ as a characteristic quantity to define the strength of the self-field relative to h, and regard $\chi_{\rm ini}=-0.5$ as a critical

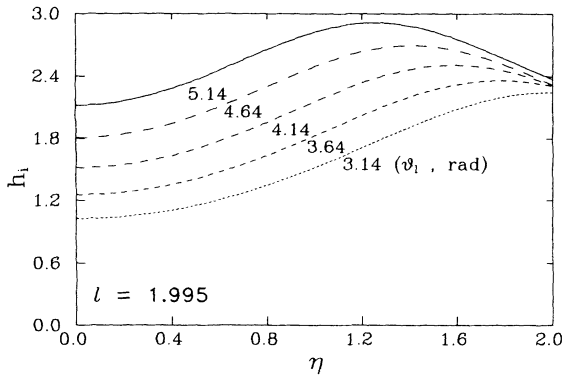

FIG. 8. The $h_i(\eta)$ profiles of a junction with $l=l_c$ when $\theta_l=3.14$, 3.64, 4.14, 4.64, and 5.14.

value at which both fields have balanced influences. Using Eq. (11), this leads to a critical l, $l_c'=1.915$.

In terms of JVs, such a low-field shielding state is a vortex state of $n_v \ll 1$. With increasing h, n_v increases, and a greater fraction of JV enters the JJ from the edge. The shielding state ends at $n_v=0.5$ with $\theta_l=\pi$, where the h_i takes its maximum value h at the edge and decreases monotonically with $\eta\to 0$. When $n_v \gtrsim 0.5$, h_i near the edge will be greater than h; i.e., part of the JVs starts to reinforce the magnetization. This feature is common for all JJs. However, there is a qualitative difference between shorter and longer JJs. For the former, a continuous flux increase (θ_l increase) during the first JV entry requires an increase in h, since the flux of the JVs is mainly provided by h; for the latter, however, the same flux increase requires a decrease in h during the JV entry, since the flux carried by the JVs is mainly produced by the vortex currents (or contributed by the self-field), and the entry of JVs itself already brings in overly large flux. These two cases are separated by $l=l_c$, where h remains constant at a certain moment during the flux entry. Several $h_i(\eta)$ profiles for $l=l_c$ are given in Fig. 8 to illustrate this situation.

Since both l_c and l_c' are very close to 2, this should serve as an unambiguous boundary between the self-field and applied-field dominated JJs. If we further calculate $\chi_{\rm ini}$ as a function of l using Eq. (11), we will find that the traditional short JJs with $l<0.5$ corresponds to $\chi_{\rm ini}>-0.076$. Symmetrically, we can define very long JJs using $\chi_{\rm ini}<-0.924$, which leads to $l>13$. Thus, with increasing l, JJs can be short ($l<0.5$), long reversible ($0.5<l<2$), long irreversible ($2<l<13$), and very long ($l>13$). Such classifications work well for low h; the relative self-field effect weakens with increasing h, and at sufficiently high h the properties of longer JJs will approach those of shorter ones.

D. Hysteresis loop

When $l>l_c$, starting from the state where $m=h=0$ and increasing h, the magnetic state will move reversibly along the lowest sections of the $m(h)$ curve with vertical jumps in between. Each jump corresponds to a sudden increase in JJ energy. When decreasing h from a maximum value, the state will move along the highest sections of the $m(h)$ curve with each jump corresponding to a sudden decrease in energy. Four jumps are drawn for $l=4$ in Fig. 2(d). In this example, there are two separated loops consisting of reversible sections and jumps. For greater l, such loops may be combined into one larger loop, as easily visualized from Figs. 2(e)–2(h). However, even when l is very large, there are always a few separated loops at high h, above which no more loops exist, and the magnetization curve becomes reversible.

As an example of very long JJs, $l=20$, the m oscillations become very dense, and there are 14 loops combined into one, which is similar to that of type-II superconductors (SC2s) with a surface barrier. We now focus on this situation.

As is well known, there is a thermal equilibrium $H_{\rm eq}(B)$ curve for a SC2, and the presence of a surface barrier shifts the field for vortex entry and exit to $H_{\rm en}>H_{\rm eq}$ and $H_{\rm ex}<H_{\rm eq}$ at a given B.[9,10] From a zero-field-cooled state, increasing and then decreasing H result in a hysteresis loop consisting of two linear segments with a -1 slope (if the cross-sectional dimensions are much greater than λ_L) and $M_{\rm en}(H_{\rm en})$ and $M_{\rm ex}(H_{\rm ex})$ curves.

We first consider the limit case of $l\to\infty$. Its $m_{\rm en}(h_{\rm en})$ and $m_{\rm ex}(h_{\rm ex})$ can be obtained as follows. Although n_v may take any numbers, the b/μ_0 of an infinite JJ in any case can always be regarded to be equal to the average h_i within one certain JV. Thus, we have by substituting $\theta=0$ and 2π in Eq. (6) that

$$\frac{b}{\mu_0}=\frac{2\pi}{\Delta\eta}=\frac{\pi}{kK(k)} . \tag{15}$$

Since the maximum and minimum h at a given b correspond to $\theta_l=(2i-1)\pi$ and $2i\pi$, $i=1,2,3,\ldots$, respectively, we obtain from Eq. (8a) for the JJ that

$$h_{\rm en}=2(1+a^2)^{1/2} , \tag{16}$$

$$h_{\rm ex}=2a . \tag{17}$$

Given a series of values of a, we compute b, $h_{\rm en}$, and $h_{\rm ex}$ using Eqs. (7) and (15)–(17), and then $m_{\rm en}$ and $m_{\rm ex}$ using Eq. (8b). $m_{\rm en}(h_{\rm en})$ and $m_{\rm ex}(h_{\rm ex})$ are thus obtained; they form an $m(h)$ loop, together with two straight lines with a -1 slope for $b=0$ and $b=b_{\rm max}$ (not shown), as plotted in Fig. 9. In this figure, we also give the thermal equilibrium magnetization curve $m_{\rm eq}(h_{\rm eq})$, derived by Kulik.[3] It is calculated from Eq. (15) and

$$h_{\rm eq}=4E(k)(\pi k)^{-1} , \tag{18}$$

where $E(k)$ is the complete elliptic integral of the second kind.

Three characteristic quantities at $b=0$, the lower critical field, $h_{c1}\equiv h_{\rm eq}(0)$, the first field for vortex entry, $h_{\rm en}(0)$, and the last field for vortex exit, $h_{\rm ex}(0)$, are

$$h_{c1}=4/\pi,\ h_{\rm en}(0)=2,\ h_{\rm ex}(0)=0 . \tag{19}$$

These equations can be precisely used for very long JJs.

For comparison, we give the relevant formulas for the surface barrier of SC2s that have great κ, the Ginsburg-Landau parameter. This kind of SC2s has been regarded

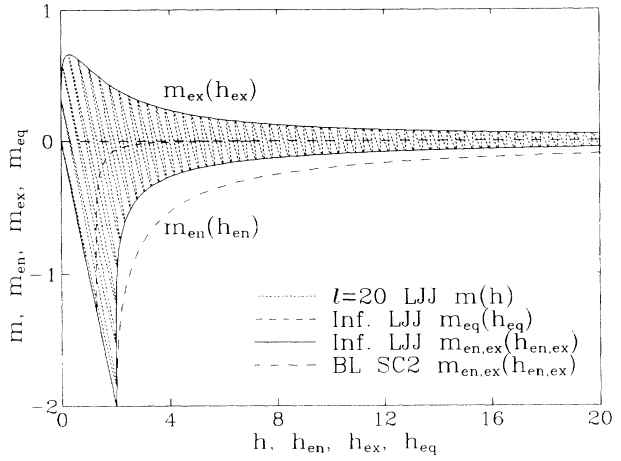

FIG. 9. The computed $m(h)$ curve for a junction with $l=20$, together with the initial magnetization curve [a line from (0,0) to (2, −2)], $m_{en}(h_{en})$ curve, $m_{ex}(h_{ex})$ curve, and $m_{eq}(h_{eq})$ curve for an infinitely long junction. Long-dashed lines give $m_{en}(h_{en})$ and $m_{ex}(h_{ex})$ curves calculated using Eqs. (20) derived in Ref. 12 for type-II superconductors.

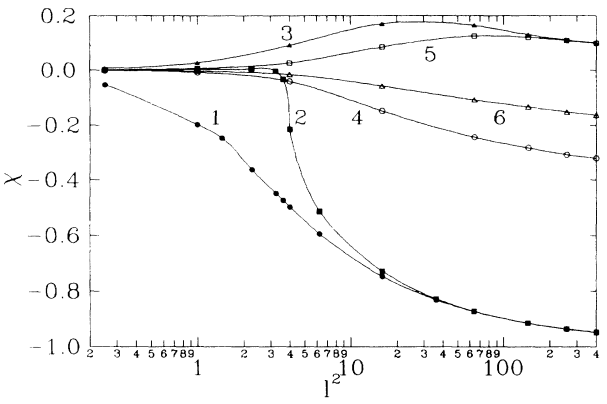

FIG. 10. χ as a function of l^2 during field cooling for $hl=2$ (1), 4.6 (2), 6 (3), 10 (4), 12 (5), and 16 (6).

as an excellent analog of long JJs. For such SC2s, we have[10]

$$H_{en}(B)\approx\sqrt{H_{en}^2+(B/\mu_0)^2},\ H_{ex}(B)\approx B/\mu_0\ . \tag{20}$$

They are much different from the results given by Eqs. (15)–(18), which have $h_{ex}\leq b/\mu_0$ and a much quicker change in h_{en} with h (see Fig. 9).

After describing the above similarities and differences between very long JJs and SC2s with a surface barrier, some other unique properties of the former are worth mentioning. (1) Their first m jump during increasing h is not from $b=0$ since $\chi_{ini}>-1$ and the initial $m(h)$ curve before the jump is not linear. (2) Each jump involves a fractional vortex entry, although the n_v change Δn_v is very close to unity at low h. (3) There is a field $h_{irr}\approx l-(\Delta h)_j$ above which no more jumps will occur, or magnetic irreversibility will disappear completely.

E. Meissner effect

We now show a great difference between JJs and SC2s concerning their Meissner effect. The Meissner effect for a superconductor is referred to as the flux expulsion in a fixed applied field H when it is being cooled down from above the critical temperature T_c. For an infinitely long ideal SC2 (without vortex pinning and surface barriers), if its transverse dimensions are much greater than λ_L at the minimum temperature, T_{min}, and $H_{c1}(T_{min})>H$, the susceptibility χ will decrease monotonically during cooling and reaches -1. If the surface barrier is considered and Eqs. (20) are valid, then the AVs can hardly exit and χ should always be close to 0. As will be seen below, the situation for JJs is much more complicated.

From the definition of the Meissner effect, we cool a JJ in a constant H. To simplify the problem we assume that the dimensions of the JJ assembly and λ_L are fixed in the temperature region of interest. Actually, the maximum possible size change is on the order of 10^{-3} even if T_c is as great as 100 K, and the assumption of fixed dimensions is justified. λ_L decreases quickly at $T\approx T_c$ and approaches a stable value when $T<T_c/2$.[11] If we are interested in low temperatures, it can be thought to be fixed; otherwise, the modification to the following results will be quantitative but not essential.

Under these assumptions, the effects of decreasing T are all due to the increase in J_0. From Eqs. (1), (2a), and (2b), we have

$$HL=\frac{\Phi_0}{4\pi\mu_0 d}hl\ , \tag{21}$$

which means that a fixed HL is equivalent to a fixed hl. Thus, although decreasing T makes the JJ longer and modifies the $m(h)$ curve in the order from (a) to (h) in Fig. 2, the (h,m) state remains at the same hl coordinate. The h-axis length of Figs. 2(a)–2(h) is actually designed following this rule. Moreover, this state must move continuously without any jump, which is energetically unfavorable. Thus, fixing a value of hl, we can get a number of (h,m) states located on the $m(h)$ curves in Fig. 2 and some others that are not shown, from which the susceptibility $\chi=m/h$ is calculated. Such a χ is plotted as a function of l^2 in Fig. 10 for different values of hl. From Eqs. (1) and (2a),

$$l^2=\frac{4\pi\mu_0 dL^2}{\Phi_0}J_0\ , \tag{22}$$

which is a measure of J_0. Knowing the relation between J_0 and T, the $\chi(l^2)$ function is readily reconstructed to a $\chi(T)$ function more relevant for the Meissner effect.

We observe from Fig. 10 that instead of a monotonical decrease with increasing J_0 (decreasing T), χ sometimes increases. Such a unique behavior is described as follows. (1) For $hl<h_c l_c=4.63$, all $\chi(l^2)$ curves merge into one when $l^2>30$, which approaches -1 if l is very large at T_{min}; in the region $l^2<30$, χ decreases smoothly in most cases, but when hl is close to 4.63, it increases a little before dropping suddenly at $l^2\approx 4$. (2) For $4.63+(2i-1)\pi<hl<4.63+2i\pi$, $i=1,2,3,\ldots$, χ decreases with increasing l^2. (3) For

$4.63+(2i-2)\pi < hl < 4.63+(2i-1)\pi$, $i=1,2,3,\ldots$, χ shows a positive peak. (4) The total χ change in cases (2) and (3) decreases with increasing i; when $i=1$, the lowest χ in case (2) is close to -0.35, and the χ peak in case (3) is a little less than 0.2.

A Meissner effect similar to that of ideal SC2s occurs in case (1). Changing back to unnormalized quantities, the condition for this effect to take place is

$$\Phi_J \equiv 4\mu_0 dLH < \frac{4.63}{\pi}\Phi_0 = 1.47\Phi_0 . \tag{23}$$

That is, if the flux within the JJ and produced by H is less than $1.47\Phi_0$, the effect is normal in the sense of $\chi \to -1$. However, even in this case, there is a big difference between the JJ and the SC2. The upper limit of H for ensuring such an effect in a JJ is very small. Using the normalized quantities and writing the boundary field for such a Meissner effect to occur as h_{c1}^*, we have

$$h_{c1}^* = \frac{4.63}{l} = \frac{3.64}{l} h_{c1} , \tag{24}$$

which decreases with increasing l and is only 1/10 of the "thermodynamic lower critical field" h_{c1} when $l=36.4$ and $\chi_{\min} = -0.973$.

F. Essential differences between long JJs and SC2s

Up to now, we have been mainly showing the computation results of JJs concerning their magnetic properties. We have also compared them with those of SC2s occasionally. It is clear that some properties look common for both, but some others are quite different. The common ones have been emphasized in the literature, so that some important rules and concepts obtained from SC2 studies have been widely applied to JJ systems. It would also be promising in a reverse way that the rules and concepts obtained in JJ researches be used for SC2s. One would benefit more from the latter since the theoretical treatments for JJs have been made with a high precision. We have thought of all these possibilities. As a result, we conclude that although one who studies JJs can get some ideas from the existing results for SC2s or vice versa, such kind of mutual benefit is quite limited. More important now is to realize the essential differences between both.

One of the most similar features for JJs and SC2s is that their χ_{ini} is identically expressed by Eq. (11) if l denotes the half thickness normalized to λ_L of a slab for the latter. This means that both have the same low-field shielding effect characterized by their own penetration depth. At this point, a difference should not be overlooked. This effect for SC2s is due to a surface current which shields the interior up to very high fields, and a constant χ_{ini} will remain until $H = H_{\text{en}}(0)$ where first AVs enter the body. In the case of JJs, however, the shielding effect results form the fractional JV on the edge (for simiplicity we only mention a half of JJ), and the susceptibility increases continuously with increasing h during the JV entry. This looks trivial. But as will be shown below, it is this difference that makes most properties of JJs distinguished from SC2s.

Since there are both the surface current and AVs in the mixed state of SC2s, a potential barrier can exist when AVs are close to the surface, which arises from the interaction between both and forbids reversible AV entry and exit. This interaction has been treated as the surface image force. On the other hand, for very long JJs, the m jumps during the irreversible JV entry or exit cannot be ascribed to a surface barrier. Surface current merely belongs to a fractional JV, whose h_i and j profiles are always exactly the same as a part of those of the internal JVs. There is not any force other than the one due to the Gibbs potential of the entire system that acts on all the JVs. During an m jump, the entire system as a whole passes through an energy barrier related to the ac Josephson effect. In other words, the state changes from a superconducting one to another across a normal one.

Also owing to this, for SC2s, H_{ex} cannot be less than B/μ_0, since when $H = B/\mu_0$, the density of AVs reaches such a value that B becomes the same on both sides of the surface and no net image force can exist. For very long JJs, however, the h_{en} and h_{ex} are just the h corresponding to a half-edge JV and zero-edge JV, respectively. In this case, $h_{\text{ex}} < b/\mu_0$ is obvious; the former is the h_i on the JV edge and the latter is the average h_i, which is greater according to the definition of a JV stated in Sec. IV B.

In SC2s, surface barriers can be smaller than the ideal ones or even negligible, since the image force depends largely on the surface roughness. If the surface barrier effects are negligible, the configuration of AVs changes continuously with H and so does M. Therefore, the $M_{\text{eq}}(H_{\text{eq}})$ curve can be followed. In JJs, however, the same kind of thermal equilibrium $m(h)$ curve does not exist. The $m_{\text{eq}}(h_{\text{eq}})$ shown in Fig. 9 is somewhat misleading since it is not a reversible magnetization curve, and moving from one point to another along this curve would always involve m jumps if it were possible. This is another consequence of the above-mentioned difference between JJs and SC2s.

In SC2s without a surface barrier, the H_{c1} and $-M_{\text{eq}}$ increase with decreasing T so that at a given H, χ decreases continuously to -1 when H_{c1} becomes greater than H. In the ideal case of surface barrier effect,the AV exit during decreasing T occurs at $M \approx 0$ where the image force disappears, so that $\chi \approx 0$ always. In any real case, the surface barrier effect is in between, and χ decreases monotonically with decreasing T but never reaches -1, even if volume pinning does not exist. Since the continuous change in the JV configuration in very long JJs results in an oscillatory $m(h)$ curve, which can be considered as a counterpart of $M_{\text{eq}}(H_{\text{eq}})$ in SC2s, its unique "Meissner effect" is expected.

We will end this section by giving one of the essential differences between JVs and AVs. For SC2s in the mixed state, the B is traditionally considered to equal $n_L\Phi_0$, n_L being the AV line density.[11] This also requires an assumption that the surface current always shield completely the interior, contributing nothing to B, and thus each vortex current always providing a Φ_0 flux. In a JJ, there is not a separated edge current that shields completely the interior. If we regard the current belonging to

the fractional edge JV to be the counterpart of the surface current in SC2, then we will have the situation that the flux produced by each vortex is less than Φ_0. In its h_i profile, only the part above its minimum is provided by the vortex; the rest is produced by the applied field h and the edge JV.

The significance of this difference is far-reaching, whose influences on the properties of different kinds of JJ systems will be explained elsewhere. Nevertheless, we should mention here that the commonly concerned JV is actually that whose Φ_0 is almost entirely contributed by the field the current vortex produces, although in many cases, this condition has not been justified. In fact, such JVs are expressed by the soliton solution (12); they exist only in very long JJs at low fields and some strictly controlled experiments.

V. CONCLUSION

We have obtained an analytic solution, Eqs. (6)–(8), of the sine-Gordon equation (3) for a uniform JJ of length $2L$ and penetration depth λ_J, which is used for computing $m(h)$ curves and θ, h_i, and j profiles, shown in Figs. 2–6. By analyzing the results, our conclusions are as follows.

(1) JJs can be classified into short, reversible and long, irreversible and long, and very long ones, the boundary between them being $l \equiv L/\lambda_J = 0.5$, 2, and 13.

(2) JJs have the same feature as SC2s at very low fields, and their initial susceptibility is expressed by Eq. (11).

(3) When increasing and then decreasing field, the magnetization of very long JJs shows a hysteresis loop. Its irreversible parts when $l \to \infty$ are expressed by Eqs. (15)–(17), which are quantitatively different from those given in Eqs. (20) for SC2s with a surface barrier, as shown in Fig. 9.

(4) Instead of the thermal equilibrium $m_{eq}(h_{eq})$ curve introduced in the literature, the calculated $m(h)$ curve should be used for deducing reversible properties of JJs. As a consequence, the "Meissner effect" of JJs is drastically different from that of SC2s, as shown in Fig. 10.

(5) The most essential difference between JJs and SC2s is that besides the vortices there is a surface current in SC2s but not in JJs. From this, all the unique features of the magnetization of JJs can be explained by means of Josephson vortices.

ACKNOWLEDGMENTS

Preliminary work on this subject was done in collaboration with A. Sanchez. We thank F. Guinea and R. B. Goldfarb for critical comments and encouragements. This work is partially supported by Spanish CICYT through Projects Nos. MAT92-0491 and MAT92-0405.

[1] B. D. Josephson, Phys. Lett. **1**, 251 (1962); Rev. Mod. Phys. **36**, 216 (1964); Adv. Phys. **14**, 419 (1965); in *Superconductivity*, edited by R. D. Parks (Marcel Dekker, New York, 1969), Vol. 1, p. 423.

[2] R. A. Ferrell and R. E. Prange, Phys. Rev. Lett. **10**, 479 (1963).

[3] I. O. Kulik, Zh. Eksp. Teor. Fiz. **51**, 1952 (1966) [Sov. Phys. JETP **24**, 1307 (1967)].

[4] I. O. Kulik and I. K. Yanson, *The Josephson Effect in Superconductive Tunneling Structures* (Nauka, Moskva, 1970; Israel Program for Scientific Translations Ltd., 1972), p. 45.

[5] C. S. Owen and D. J. Scalapino, Phys. Rev. **164**, 538 (1967).

[6] A. A. Abrikosov, *Fundamentals of the Theory of Metals* (North-Holland, Amsterdam, 1988), p. 552.

[7] T. Yamashita and L. Rinderer, J. Low Temp. Phys. **21**, 153 (1975).

[8] J. R. Clem, Physica C **153-155**, 50 (1988).

[9] C. P. Bean and J. D. Livingston, Phys. Rev. Lett. **12**, 14 (1964).

[10] J. R. Clem, in *Low Temperature Physics-LT 13*, edited by K. D. Timmerhaus *et al.* (Plenum, New York, 1974), p. 102.

[11] P. G. de Gennes, *Superconductivity of Metals and Alloys* (Addison-Wesley, Redwood City, CA, 1989), pp. 26 and 65.